Microporous and Mesoporous Materials 275 (2019) 26–30

Contents lists available at ScienceDirect

Microporous and Mesoporous Materials

journal homepage: www.elsevier.com/locate/micromeso

The influence of ethanol-assisted washes to obtain swollen and pillared MWW-type zeolite with high degree ordering of lamellar structure

Anderson Joel Schwanke[a,*], Urbano Díaz[b], Avelino Corma[b], Sibele Pergher[a]

[a] Universidade Federal do Rio Grande do Norte, Laboratório de Peneiras Moleculares, 59078-970, Natal, RN, Brazil
[b] Instituto de Tecnología Química, Universitat Politècnica de València-Consejo Superior de Investigaciones Científicas, 4602, Valencia, Spain

ARTICLE INFO

Keywords:
Ethanol extraction
MWW
MCM-22
Swelling
Pillaring
Hierarchical zeolites

ABSTRACT

We studied the influence of the ethanol used as a washing solvent for obtaining swollen and pillared MWW topology zeolites with long-range ordering of lamellar structure. The diffractogram results showed that the increased number of washes increases the degree of order of the lamellar structure. Thermogravimetric results showed a considerable removal of the weakly interacting surfactant molecules after the third wash. The washes with ethanol did not remove the surfactant that strongly interacted with the MWW structure. The pillared material after the third wash showed a long-range ordering of the lamellar structure with the surface area of 728 $m^2 g^{-1}$, mesopore sizes of 2–4 nm and morphology characteristic of pillared MWW-type zeolites.

1. Introduction

Zeolites are a class of microporous crystalline materials formed by the tetrahedral (Si Al, P, Ti, Ge, Ga, Fe, Nb, etc.) units linked by oxygen atoms and widely used as catalysts, adsorbents, molecular sieving materials, ion-exchangers and supports [1,2]. According to the International Zeolite Association, there are more than 230 zeolite topologies, with most of them showing tridimensional structures obtained by direct synthesis or after calcination [3]. On the other hand, few topologies form lamellar zeolitic precursors (LZPs) propagated in only two dimensions [4]. The LZPs offer great versatility for creation of open pore structures (pillared, exfoliated, disordered, desilicated, hybrid) with improved access for larger molecules compared to the microporous zeolite channels (less than 1 nm) [5–8]. Among the best example of lamellar zeolitic precursors, the LZP of the MCM-22 (MWW topology) zeolite is the most versatile for post-synthetic modifications. The LZP of the MWW zeolite possesses sinusoidal 10-ring channels and 12-ring hemicavities on the external surface, and after its calcination of LZP, the silanol groups are condensed on the surface of the MWW lamellae and form internal supercavities by the union of hemicavities through 10-ring windows [5].

To obtain open lamellar pore structures and in particular the pillared-MWW materials, the individual MWW lamellae of the LZP are separated with a swelling procedure using cationic surfactants in high pH media [9]. The intercalation chemistry involves the deprotonation of the silanol groups ($\equiv Si-O^-$) on the surface of each MWW lamellae. The negatively charged groups on the surface of MWW lamella repel each other, and simultaneously, attract the cationic surfactant molecules that fill the interlamellar region [10]. Consecutively, a pillaring agent, such as tetraethylorthosilicate (TEOS), is added, and rigid SiO_2 pillars are stabilized after calcination. The MCM-36 was the first pillared zeolite with a hierarchical structure of mesopores (interlamellar regions between MWW lamellae) and micropores (of each individual lamella). This MWW-type pillared material showed higher adsorption capacities for bulky hydrocarbon molecules, enzymes, and catalytic activity than the microporous MCM-22 zeolite [11–13].

However, the swelling procedure of the LZP of the MWW-type materials is still considered to be a complex procedure with a stoichiometry that is not completely defined and has a high cost and is time consuming [11,14,15]. These factors are still challenging for the large-scale implementation of lamellar zeolites with open pore architectures. Thus, several efforts have been focused on obtaining a better understanding of the transition between swollen and pillared MWW-type materials as well as the more economical and environmentally friendly routes for obtaining the MWW-type materials. The swelling procedure was studied using soft (25 °C) or aggressive (80 °C) treatments showing that structural integrity and long-range ordering of the lamellar structure were obtained with soft swelling procedure [16]. Recently, we reported the influence of molecular dimensions of swelling agents ($C_{12}TA^+$, $C_{16}TA^+$, $C_{18}TA^+$) combined with soft and aggressive swelling

* Corresponding author.
E-mail addresses: anderson-js@live.com, andersonjoelschwanke@gmail.com (A.J. Schwanke), udiaz@itq.upv.es (U. Díaz), acorma@itq.upv.es (A. Corma), sibelepergher@gmail.com (S. Pergher).

https://doi.org/10.1016/j.micromeso.2018.08.010
Received 26 March 2018; Received in revised form 31 July 2018; Accepted 10 August 2018
Available online 14 August 2018
1387-1811/

procedures to obtain tunable properties such as surfactant accommodation between lamellae, the surface area, pore sizes and acidic nature [7]. Furthermore, an economical and eco-friendly procedure based on the reuse of the recyclable swelling solution was reported and showed that it is possible to obtain swollen MWW-type LZP three times without compromising the physicochemical properties of the pillared material [17].

Another procedure is fundamental to obtain swollen and pillared materials with long-range ordering of lamellar structure. The swollen LZP must be washed to remove the excess of weakly interacting surfactant of the MWW structure. This procedure avoids the interaction of the excess of the surfactant with TEOS and the possible formation of the undesirable mesophases [18]. It was reported that this necessitates successive washes with water with a high number of centrifugation cycles from 10 to 40, at 10 000 rpm and 10 min for each cycle [16]. However, as mentioned above, the diminution of total stages to obtain swollen precursors synthesis is desirable and alternative routes to accelerate the synthesis of swollen materials with high degree of lamellar ordering still necessary.

The remove the surfactant from porous materials precursors using organic solvents are effective for this purpose. Furthermore, the ethanol is the most widely used organic solvent for extraction because it does not allow the complete remove of surfactant of the structure [19]. Although the economic impact of the use of ethanol can be seen negatively, the fact that it can be separated by simple solvent distillation for reuse opens up the possibility of its application. Indeed, the use of washing solvents for partial or total surfactant removal and reuse was reported for some porous materials such as MCM-41, SBA-15 and HMS [20–22]. In other cases, the remaining surfactant interacted with the inorganic structure served to adsorb molecules of specific interest [23,24]. To the best of our knowledge, there are no alternative procedures for the partial removal of a surfactant from swollen MWW-type zeolites in the current literature. Here, we explore the influence of the use of ethanol as a washing solvent with a simple alternative to the successive cycles of washes and centrifugation to obtain swollen and pillared MWW-type materials.

2. Experimental

2.1. Synthesis of MWW-type LZP

Synthesis of LZP precursor was carried out with the Si/Al = 25 M ratio similar to the report in the literature [25]. For the synthesis, 9.50 mmol of sodium hydroxide (NaOH, Sigma Aldrich) and 4.51 mmol of sodium aluminate ($NaAlO_2$, Riedel de-Haën) were added to 4.51 mol distillated water under magnetic stirring. Then, 50.22 mmol of hexamethyleneimine (HMI (Sigma Aldrich) and 100 mmol of fumed silica (SiO_2, Aerosil 200, Degussa) were added to the mixture and stirred for 2 h. Then, the resulting gel was added to a Teflon-lined stainless-steel autoclave under rotation autoclaves (60 rpm) at 135 °C for 7 days. The autoclaves were quenched, and the resultant solid was filtered with deionized water until the pH was close to 7. The LZP was dried at 60 °C for 12 h. The tridimensional zeolite MCM-22 used as the reference was obtained after the calcination of LZP at 580 °C for 18 h and was named 3*D* MCM-22.

2.2. Swelling of LZP

Swelling of the LZP was similar to the procedure reported in the literature [7]. The swelling LZP was carried out at room temperature with 1.80 g of LZP, 7.20 g of distilled water, 35.00 g of an aqueous solution of 29 wt% CTABr/OH with 51% of ionic exchange and 11.0 g of an aqueous solution of 40 wt% TPABr/OH with 45% of ionic exchange. The mixture was magnetically stirred for 18 h and the swollen LZP was separated by centrifugation (12 000 rpm, 10 min) and named Sw. The washes were performed with absolute ethanol (Sigma Aldrich) with the weight ratio of swollen LZP/ethanol = 0.8. at 25 °C with magnetic stirring (300 rpm) for 1 h and centrifugation. The repetitions were done with fresh ethanol and named according to the number of washes, E_1, E_2, E_3 E_4 and E_5.

2.3. Pillaring of swollen LZP

The pillaring procedure was carried out at 80 °C for 24 h with magnetic stirring under nitrogen atmosphere and the weight ratio of swollen LZP/TEOS (Sigma Aldrich) was 0.2. The obtained material was calcined at 540 °C (rate 3 °C min^{-1}) under N_2 flow (1 mL s^{-1}) and synthetic air (1 mL s^{-1}) for 8 h. The pillared sample has the suffix “pil”.

2.4. Characterization

The XRD patterns of obtained materials were analyzed with a PANalytical Cubix fast diffractometer using Cu-Kα1 radiation and an X'Celerator detector in the Bragg-Brentano geometry in the regions of 2Θ = 2–30°. The XRD pattern in the low-angle region of 2ϴ = 1–30° were recorded with a Rigaku Ultima IV using Cu-Kα1 radiation.

Nitrogen adsorption isotherms at −196 °C were measured with a Micromeritics ASAP 2010. Prior to the analysis, the samples were outgassed for 12 h at 300 °C. The specific surface area (S_{BET}) was calculated by the BET method from the nitrogen adsorption data in the relative pressure range from 0.06 to 0.11. The external surface area (S_{ext}) was estimated using the t-plot method. The total pore volume (*VTP*) was obtained from the adsorbed amount of N_2 at the relative pressure of approximately 0.99. The pore size distribution (*PSD*) was obtained using the BJH method with nitrogen adsorption branch data.

Elemental analyses were performed by inductively coupled plasma optical emission spectrometry (ICP-OES) on a Varian 715-ES instrument after the dissolution of the samples in a HNO_3/HF solution.

Thermogravimetric analyses (TGA/DTG) were determined by a Mettler-Toledo SDTA851E analyzer in air flux with the heating range of 10 °C min^{-1}.

Transmission electron microscopy analyses (TEM) were recorded on a Philips CM10 operating at 100 kV. Scanning electron microscopy (SEM) analyses were recorded with a JEOL JSM6300 at 30 kV using backscattered electron detector.

3. Results and discussion

Fig. 1 shows the XRD patterns of LZP, the swollen sample and after

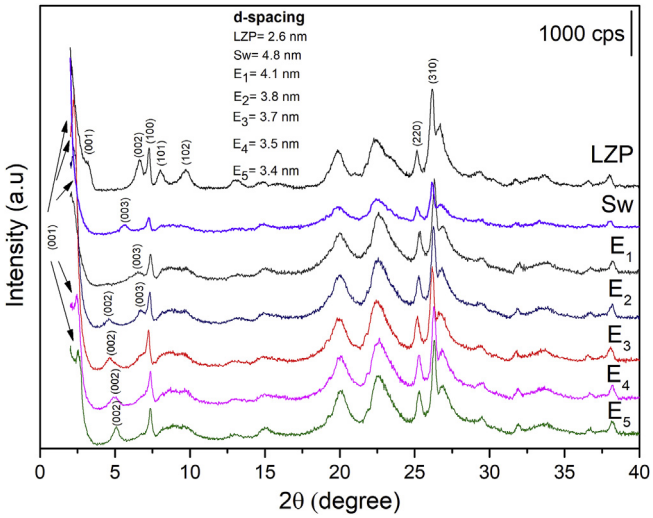

Fig. 1. XRD patterns of LZP and swollen material (Sw) and after the washes with ethanol, E_1, E_2, E_3, E_4, and E_5.

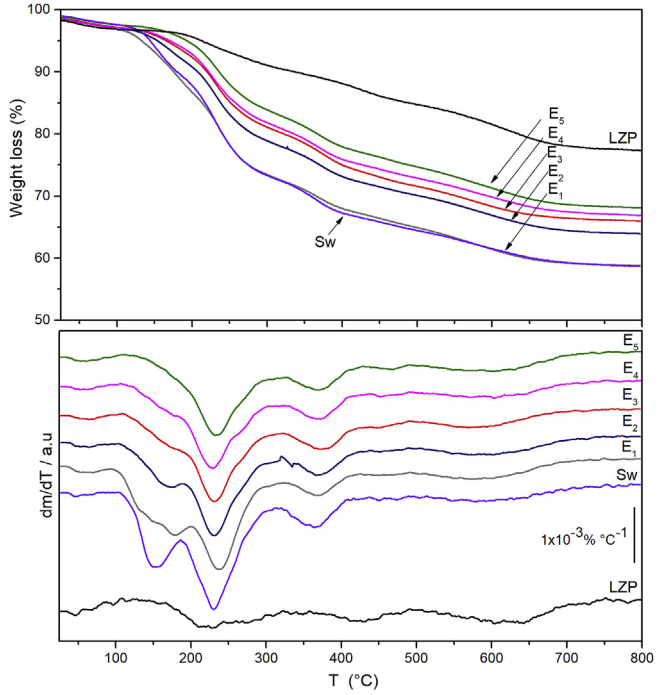

Fig. 2. TGA/DTG analyses of swollen material (Sw) and after the washes with ethanol E_1, E_2, E_3, E_4, and E_5.

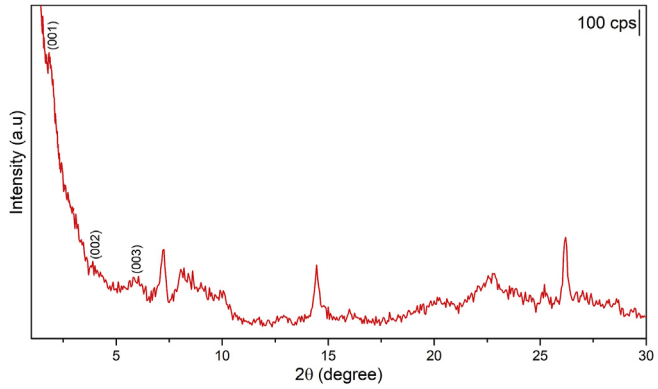

Fig. 3. XRD pattern of pillared sample E_3-pil.

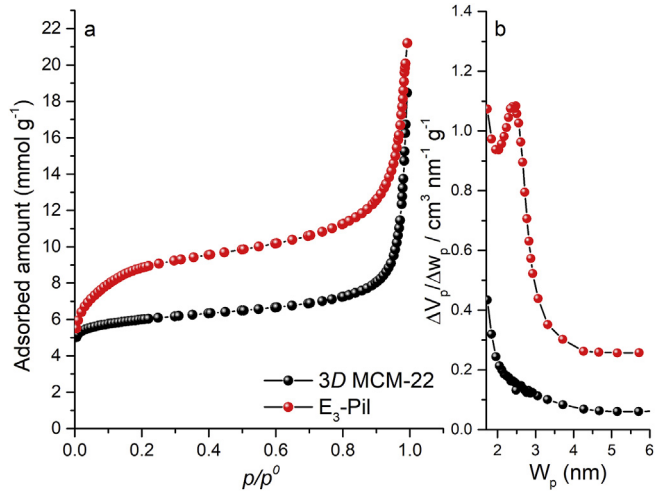

Fig. 4. Nitrogen adsorption isotherms (a) and pore size distribution (b) of samples the E_3-pil and 3*D* MCM-22.

five washes with ethanol. The main difference between the LZP and swollen samples is the overlap of the (101) and (102) reflections to a broadband and the shift of the (00l) diffraction bands to low angles, which is characteristic of the swollen samples [26]. In addition, the (002) reflection emerges after the second extraction (E_2) and indicates the long-range ordering of stacking of the MWW lamellae. By contrast, it is reported that the traditional procedure requires 20 cycles of centrifugation and redispersion in fresh water to observe the emergence of the (002) reflection of the swollen material [16].

The slight shift of the (00l) diffraction planes at high angles indicated a slight decrease of the d-spacing with the increased number of washes. It was noted that (003) peak did not disappear but is gradually overlapped by the intralamellar (100) diffraction plane after the second wash. Furthermore, all (100), (220) and (310) diffraction planes characteristic of the intralamellar MWW zeolitic structure were maintained. The measured pH of the starting swelling mixture was 13.60 and did not decrease after the ethanol washes.

The amount of the organic content after each wash was monitored by TGA/DTG analysis and is shown in Fig. 2 (weight loss values for each event are in Table 1A, Appendix). Generally, the organic content decreases with the increasing number of washes. The samples Sw, E_1, E_2, E_3, E_4, E_5 and LZP showed the total weight loss values of, 41, 39, 39, 32, 31, 30 and 20 wt%, respectively. The first weight loss event of samples (25–110 °C) was attributed to the physically adsorbed water and ethanol the content of which decreased after swelling due the hydrophobic surfactant chains of the swelling agents. The second event (110–180 °C) is associated with the surfactant weakly interacting with the MWW structure or located outside of the interlamellar region. A decrease of this peak with the increased number of washes was observed. The weight loss values showed an abrupt decrease of the organic content after the second and third washes, from 9.39 to 3.79 wt%, respectively. This indicate a considerable removal of the weakly interacted surfactant.

The event between 180 and 340 °C is associated with the oxidation of the swelling agents located in the interlamellar region and the HMI molecules in the 12-ring hemicavities of the MWW surface. In addition, the weight loss values of the swollen samples between the first and fifth washes ranged from 14.85 to 13.00 wt%, respectively. These results indicate that ethanol did not remove a considerable amount of the strongly interacting surfactant between the interlamellar regions with the increase of the washes. The weight loss event in the 340–480 °C range is associated with the oxidation of the HMI molecules in the sinusoidal 10-ring channels of the individual MWW lamellae. The weight loss events above 480 °C were associated with the residual organic molecules (surfactant and HMI) and water produced by the condensation of the silanol groups present on the surface of the MWW lamellae [7]. Both events have similar values for swollen and extracted samples and indicate that only the weakly interacting surfactant molecules were considerably removed. The LZP showed a total weight loss of 20 wt% and different weight loss events compared with the swollen and extracted samples. The event between 110 and 340 °C is characterized by oxidation of HMI molecules in the 12-ring hemicavities of the MWW surface while the event between 340 and 500 °C is attributed to the oxidation HMI molecules in 10-ring sinusoidal channels of each individual MWW lamella. The event between 500 and 800 °C is characterized by the oxidation of residual HMI content and dehydroxylation of silanol groups. When the DTG of the LZP and the swollen and washed samples were compared, the last two weight loss events of swollen and washed samples occurred in lower temperatures than LZP because the swelling procedure break some MWW lamellae structure and the HMI molecules are more easily oxidized.

The XRD patterns in Fig. 1 shows the increase of the (00l) diffraction bands characteristic of long-range ordering of the lamellar structure after the second wash. In addition, TGA/DTG results shown in Fig. 2 demonstrated that the weakly interacting surfactant was removed after the third wash. Thus, the E_3 sample was chosen for pillaring and its XRD

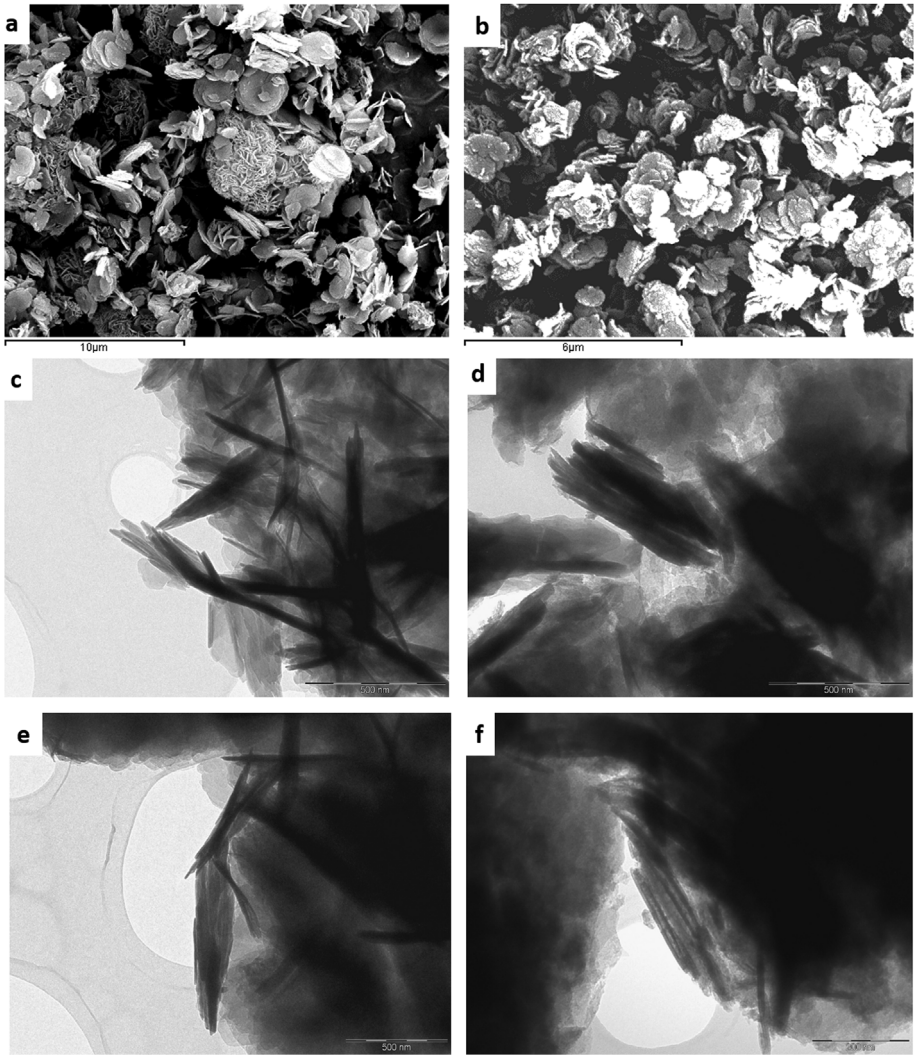

Fig. 5. SEM images of samples (a) LZP, (b) E_3-pil and TEM images of (c) and (e) LZP and (d) and (f) E_3-pil.

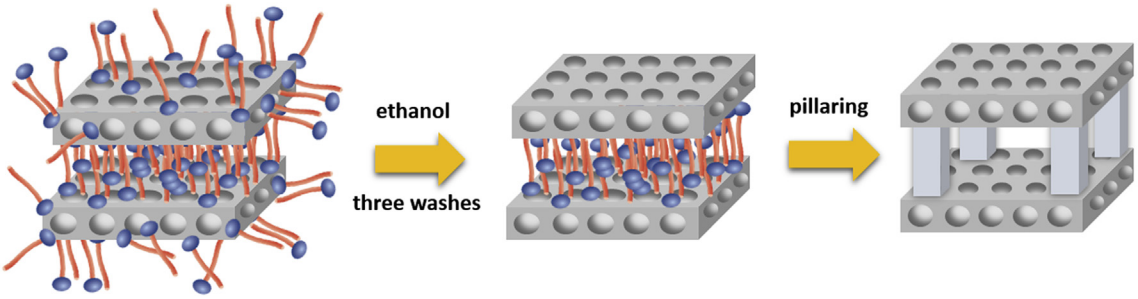

Fig. 6. Scheme of swollen MWW-type materials after ethanol-assisted washes and pillaring.

pattern is shown in Fig. 3. The diffractogram showed the (00l) diffraction planes of second and third order, indicating a long-range ordering of the lamellar structure. In addition, the coalescence of the (101) and (102) diffraction peaks into a broadband reflection was maintained and indicates that the MWW lamellae were separated. The d-spacing of 4.6 nm indicates the interlamellar region of 2.1 nm (d-spacing subtracted from the thickness of an individual MWW lamella, 2.5 nm). The ICP results for E_3 and E_3-Pil samples showed the increase of the Si/Al ratio from 18 to 35, respectively, confirming that silica pillars were stabilized after calcination.

Fig. 4 shows the nitrogen adsorption isotherms and PSD of E_3-pil and the tridimensional zeolite, 22. The E_3-pil showed a higher amount of nitrogen adsorbed at low pressures compared to the 3*D* MCM-22 sample. In addition, the pressures for p/p^0 of 0.1–0.4 indicate the presence of capillary condensation phenomena in the mesopores after the pillaring. The 22 sample showed a type-I isotherm which is characteristic of microporous materials where the high nitrogen capacity adsorbed occurred at pressures $p/p^0 < 0.1$. Fig. 4 (image b) showed the *PSD* of synthesized materials and the E3-pil sample showed pore regions between the supermicropores and small mesopores (2–4 nm), corroborating the XRD results. The BET surface area of E_3-pil is 728 $m^2 g^{-1}$ when compared with 446 $m^2 g^{-1}$ for the 3*D* MCM-22 sample. In addition, the S_{ext} showed the values of 373 $m^2 g^{-1}$ for the E_3-pil sample, which is higher than the 3*D* MCM-22 sample with 120 $m^2 g^{-1}$. These

values indicate the high accessibility of the pillared sample.

SEM images of LZP and E_3-pil samples are shown in Fig. 5 (images a and b, respectively), and it can be seen that the crystals of E_3-pil are less smooth than LZP due to swelling and pillaring treatments. However, hexagonal flake-like crystals with 1.4 μm are observed for both samples, and no morphology of other mesophases were observed. TEM analysis of the E_3-pil (image d) showed more expanded MWW particle crystals when compared to the flat crystals of LZP (image c). Image e (see yellow circle) showed regions of low-density between the dark regions (MWW crystals), which is attributed to the interlamellar expansion after swelling and pillaring procedures. On the other hand, it is not possible to observe regions with low densities between the crystals of the LZP (image e). The scheme in Fig. 6 summarizes the swollen, pillared MWW-type zeolite and the removal of the weakly interacted surfactant after ethanol-assisted washes.

4. Conclusions

An alternative procedure to obtain swollen and pillared MWW-type materials with long-range ordering of lamellar structure using ethanol as the washing solvent was reported. It was demonstrated that (002) and (003) diffraction planes are obtained showing a high degree of ordering of the lamellar stacking after the second wash. The thermogravimetric analyses showed that weakly interacted surfactants were substantially removed after the third wash. The pillared material maintained the high degree of lamellar stacking, with d-spacing of 4.6 nm, surface area of 728 $m^2 g^{-1}$ and pores sizes between 2 and 4 nm. These results confirm that washes of ethanol serve as an alternative route to the successive repetitions of washes with high centrifugation cycles commonly used to obtain MWW materials with a high order of degree of the lamellar structure.

Acknowledgements

Anderson Joel Schwanke is grateful the CAPES Foundation and PDSE program (process number 99999.004779/2014–02). Urbano Díaz acknowledges to the Spanish Government (MAT2014-52085-C2-1-P and MAT2017-82288-C2-1-P).

Appendix A. Supplementary data

Supplementary data related to this article can be found at https://doi.org/10.1016/j.micromeso.2018.08.010.

References

[1] A. Corma, Chem. Rev. 97 (1997) 2373–2420.
[2] J. Weitkamp, L. Puppe, Catalysis and Zeolites: Fundamentals and Applications, first ed., Springer, Berlin, 1999.
[3] IZA, International Zeolite Association, web page http://www.iza-structure.org/.
[4] W.J. Roth, P. Nachtigall, R.E. Morris, J. Čejka, Chem. Rev. 114 (2014) 4807–4837.
[5] U. Diaz, A. Corma, Dalton Trans. 43 (2014) 10292–10316.
[6] A. Corma, V. Fornes, S.B.C. Pergher, T.L.M. Maesen, J.G. Buglass, Nature 396 (1998) 353–356.
[7] A.J. Schwanke, S. Pergher, U. Díaz, A. Corma, Microporous Mesoporous Mater. 254 (2017) 17–27.
[8] A. Corma, U. Díaz, T. García, G. Sastre, A. Velty, J. Am. Chem. Soc. 132 (2010) 15011–15021.
[9] C.T. Kresge, W.J. Roth, K.G. Simmons, J.C. Vartuli, WO1992011934 A1 patent, 1992.
[10] W.J. Roth, Pol. J. Chem. 80 (2006) 5.
[11] W.J. Roth, C.T. Kresge, J.C. Vartuli, M.E. Leonowicz, A.S. Fung, S.B. McCullen, H.G.K.I.K.H.K. Beyer, J.B. Nagy (Eds.), Stud. Surf. Sci. Catal, Elsevier, New York, 1995, pp. 301–308.
[12] E. Dumitriu, F. Secundo, J. Patarin, I. Fechete, J. Mol. Catal. B Enzym. 22 (2003) 119–133.
[13] E.J.A. Schweitzer, van der P.F. Oosterkamp, Microporous Mesoporous Mater. (1998) 20.
[14] W.J. Roth, J. Cejka, Catal. Sci. Technol. 1 (2011) 43–53.
[15] J. Čejka, G. Centi, J. Perez-Pariente, W.J. Roth, Catal. Today 179 (2012) 2–15.
[16] S. Maheshwari, E. Jordan, S. Kumar, F.S. Bates, R.L. Penn, D.F. Shantz, M. Tsapatsis, J. Am. Chem. Soc. 130 (2008) 1507–1516.
[17] A.J. Schwanke, U. Díaz, A. Corma, S. Pergher, Microporous Mesoporous Mater. 253 (2017) 91–95.
[18] M.V. Opanasenko, W.J. Roth, J. Cejka, Catal. Sci. Technol. 6 (2016) 2467–2484.
[19] J. Gonzalez-Rivera, J. Tovar-Rodríguez, E. Bramanti, C. Duce, I. Longo, E. Fratini, I.R. Galindo-Esquivela, C. Ferrari, J. Mater. Chem.A 2 (2014) 7020–7033.
[20] N. Lang, A. Tuel, Chem. Mater. 16 (2004) 1961–1966.
[21] S.G. de Ávila, L.C.C. Silva, J.R. Matos, Microporous Mesoporous Mater. 234 (2016) 277–286.
[22] A.G.S. Prado, C. Airoldi, J. Mater. Chem. 12 (2002) 3823–3826.
[23] A. Ariapad, M.A. Zanjanchi, M. Arvand, Desalination 284 (2012) 142–149.
[24] B. Boukoussa, R. Hamacha, A. Morsli, A. Bengueddach, Arab. Journal of Chem. 10 (2017) 2160–2169.
[25] A. Corma, C. Corell, J. Pérez-Pariente, Zeolites 15 (1995) 2–8.
[26] W.J. Roth, D.L. Dorset, Microporous Mesoporous Mater. 142 (2011) 32–36.